JOURNAL OF THE AMERICAN CHEMICAL SOCIETY

Article

Journal of the American Chemical Society is published by the American Chemical Society. 1155 Sixteenth Street N.W., Washington, DC 20036

JOURNAL OF THE AMERICAN CHEMICAL SOCIETY

Amorphous Metal-Free Room-Temperature Phosphorescent Small Molecules with Multicolor Photoluminescence via a Host-Guest and Dual-Emission Strategy

Journal of the American Chemical Society is published by the American Chemical Society. 1155 Sixteenth Street N.W., Washington, DC 20036

J|A|C|S
JOURNAL OF THE AMERICAN CHEMICAL SOCIETY

Dengfeng Li, Feifei Lu, Jie Wang, Wende Hu, Xiao-Ming Cao, Xiang Ma, and He Tian

J. Am. Chem. Soc., **Just Accepted Manuscript** • DOI: 10.1021/jacs.7b12800 • Publication Date (Web): 04 Jan 2018

ACS Publications

Journal of the American Chemical Society is published by the American Chemical Society. 1155 Sixteenth Street N.W., Washington, DC 20036

JOURNAL OF THE AMERICAN CHEMICAL SOCIETY

Journal of the American Chemical Society is published by the American Chemical Society. 1155 Sixteenth Street N.W., Washington, DC 20036

JACS
JOURNAL OF THE AMERICAN CHEMICAL SOCIETY

ACS Publications

Journal of the American Chemical Society is published by the American Chemical Society. 1155 Sixteenth Street N.W., Washington, DC 20036

Journal of the American Chemical Society is published by the American Chemical Society. 1155 Sixteenth Street N.W., Washington, DC 20036
Published by American Chemical Society.

Journal of the American Chemical Society is published by the American Chemical Society. 1155 Sixteenth Street N.W., Washington, DC 20036

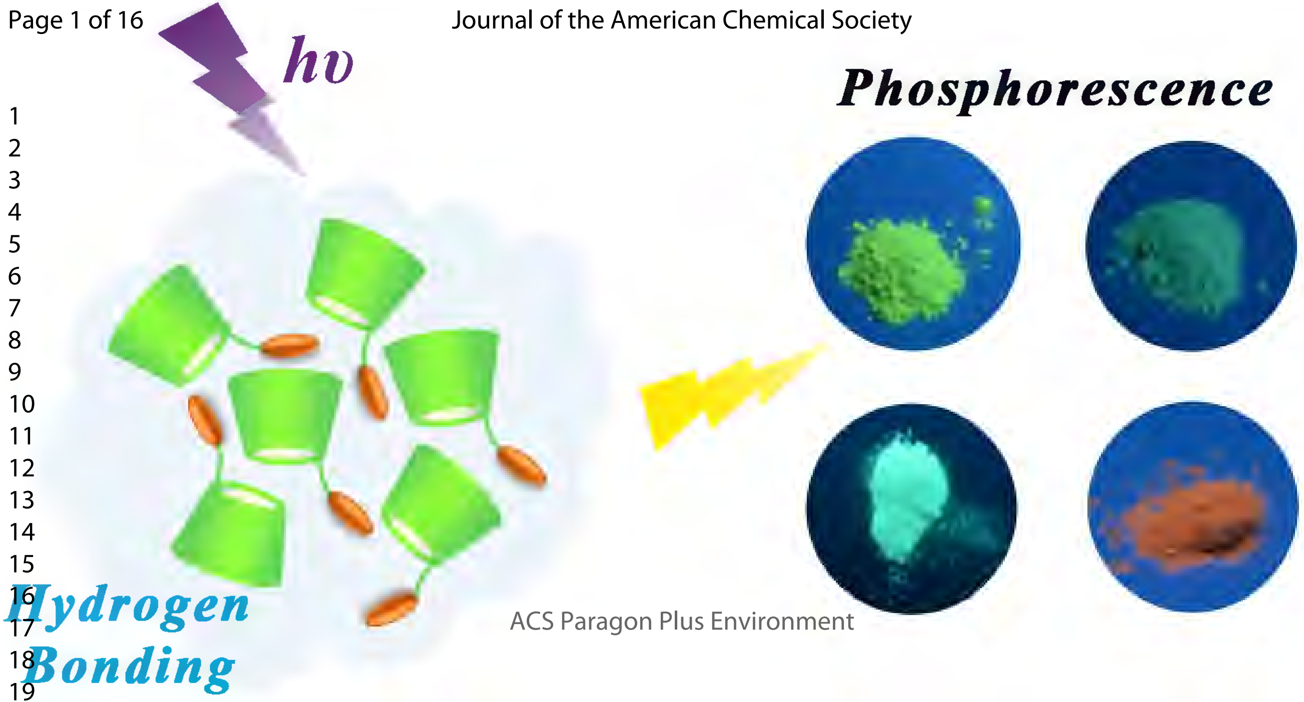
hν
Phosphorescence
Hydrogen Bonding

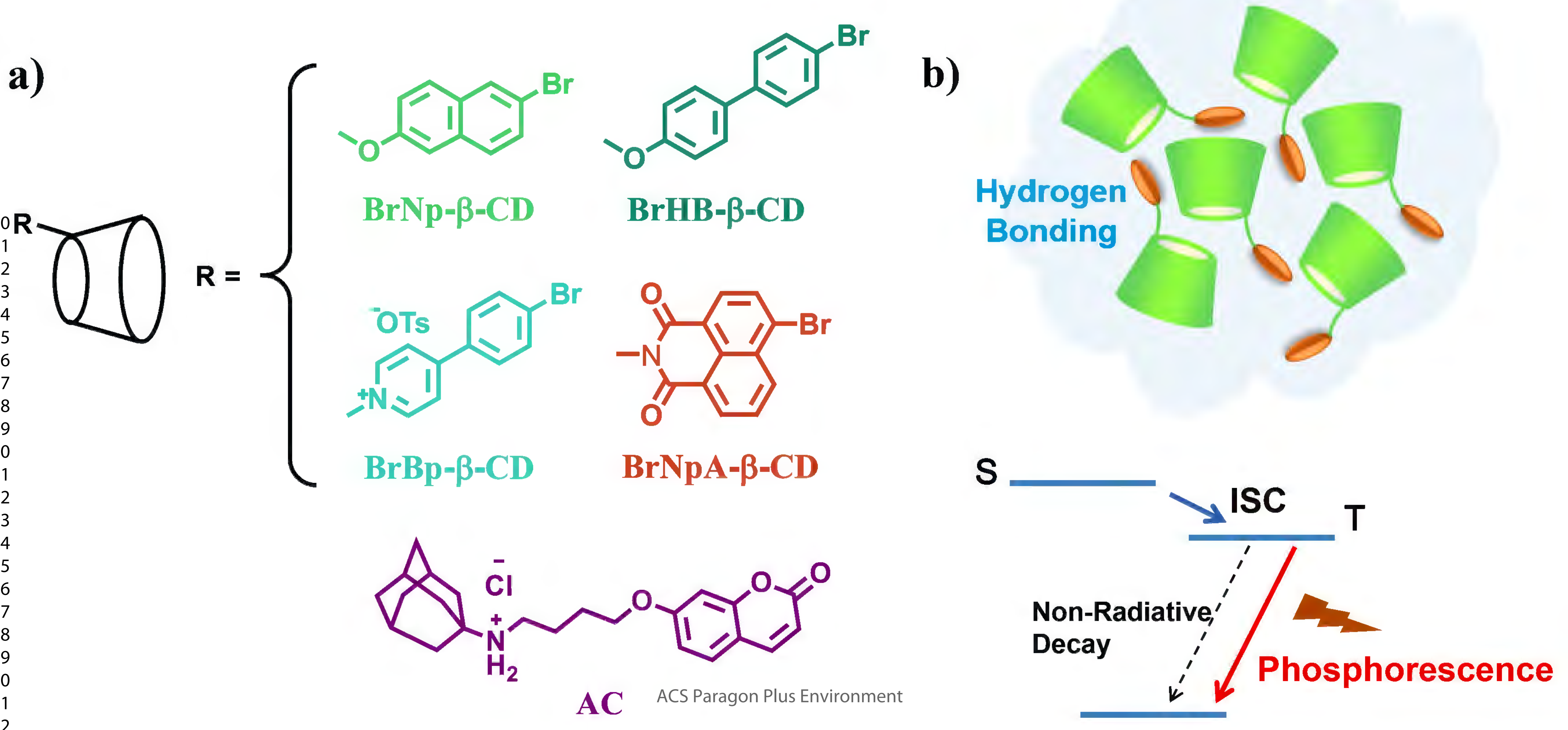
a)
R
R =
Br
O
BrNp-β-CD
Br
O
BrHB-β-CD
⁻OTs
Br
⁺N
BrBp-β-CD
O
N
O
Br
BrNpA-β-CD
Cl⁻
⁺N H2
O
O
O
AC
b)
Hydrogen Bonding
S
ISC
T
Non-Radiative Decay
Phosphorescence

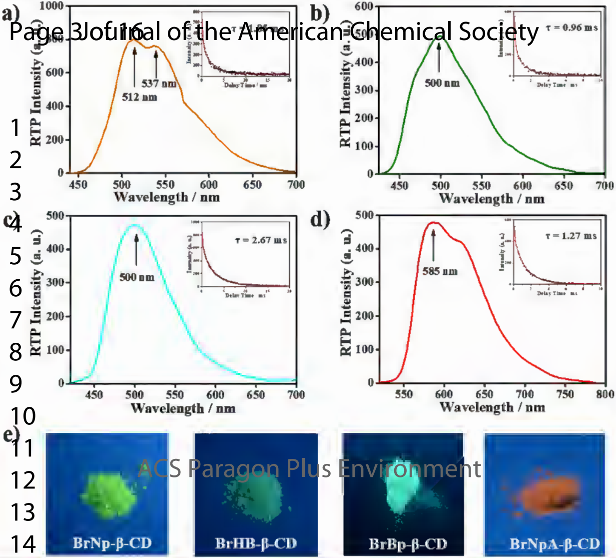
a)
RTP Intensity (a. u.)
Wavelength / nm
512 nm
537 nm
Intensity (a. u.)
Delay Time / ms
b)
500 nm
τ = 0.96 ms
c)
500 nm
τ = 2.67 ms
d)
585 nm
τ = 1.27 ms
e)
BrNp-β-CD
BrHB-β-CD
BrBp-β-CD
BrNpA-β-CD

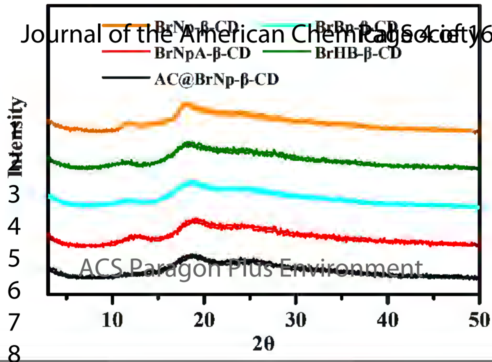
BrNp-β-CD
BrBp-β-CD
BrNpA-β-CD
BrHB-β-CD
AC@BrNp-β-CD
Intensity
10
20
30
40
50
2θ

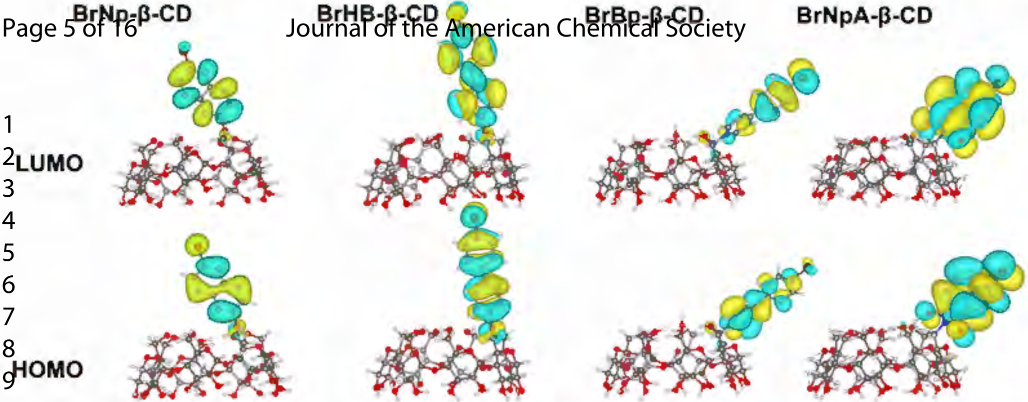

	BrNp-β-CD	BrNp	BrHB-β-CD	BrHB	BrBp-β-CD	BrBp	BrNpA-β-CD	BrNpA
S_1 /eV	3.92	3.77	4.17	4.09	3.84	3.37	3.19	3.93
T_1 /eV	2.29	2.32	2.60	2.57	2.64	1.97	1.95	2.67
ΔE_{ST}/eV	1.62	1.45	1.58	1.52	1.19	1.41	1.25	1.25

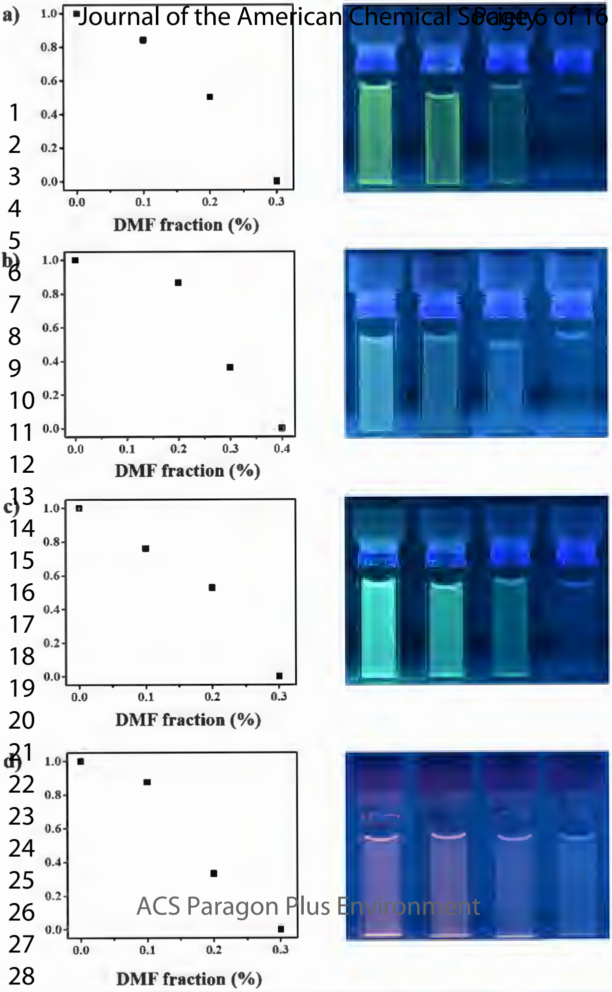
a)
1.0
0.8
0.6
0.4
0.2
0.0
0.0
0.1
0.2
0.3
DMF fraction (%)
b)
1.0
0.8
0.6
0.4
0.2
0.0
0.0
0.1
0.2
0.3
0.4
DMF fraction (%)
c)
1.0
0.8
0.6
0.4
0.2
0.0
0.0
0.1
0.2
0.3
DMF fraction (%)
d)
1.0
0.8
0.6
0.4
0.2
0.0
0.0
0.1
0.2
0.3
DMF fraction (%)

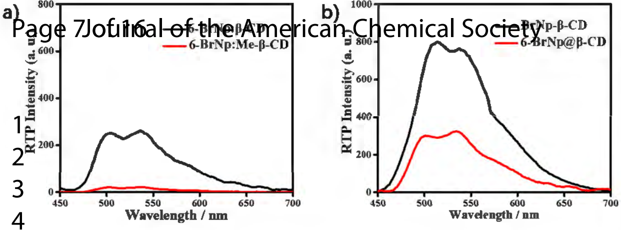

c)

	BrNp-β-CD	6-BrNp@β-CD	6-BrNp:β-CD	6-BrNp:Me-β-CD
T_p(ms)	1.85	1.69	1.65	1.54
Φ_p(%)	5.9	2.9	1.0	<0.1

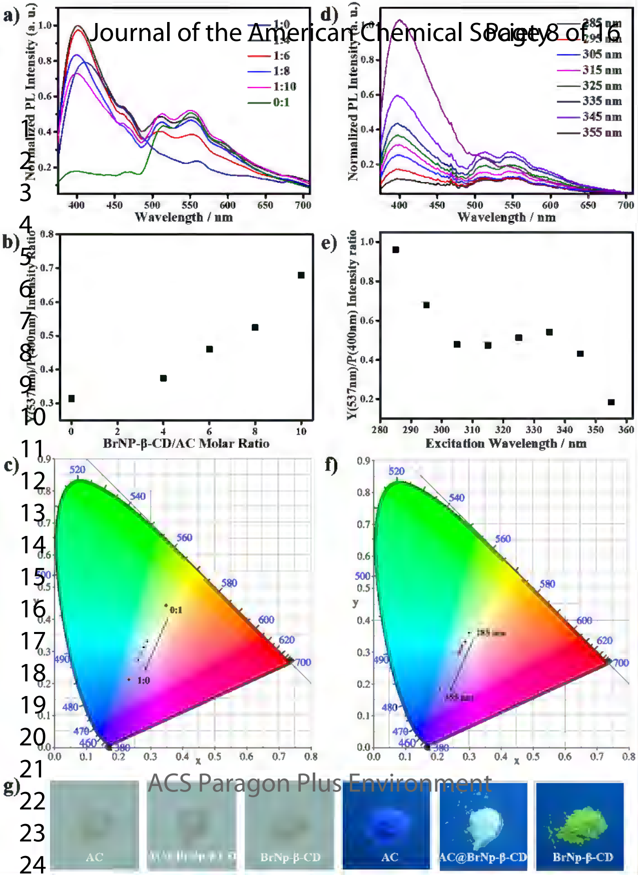
a)
Normalized PL Intensity (a. u.)
Wavelength / nm
1:0
1:4
1:6
1:8
1:10
0:1
d)
Normalized PL Intensity (a. u.)
Wavelength / nm
285 nm
295 nm
305 nm
315 nm
325 nm
335 nm
345 nm
355 nm
b)
Y(537nm)/P(400nm) Intensity Ratio
BrNP-β-CD/AC Molar Ratio
e)
Y(537nm)/P(400nm) Intensity ratio
Excitation Wavelength / nm
c)
0:1
1:0
x
y
f)
285 nm
355 nm
x
y
g)
AC
AC@BrNp-β-CD
BrNp-β-CD
AC
AC@BrNp-β-CD
BrNp-β-CD

Amorphous Metal-Free Room-Temperature Phosphorescent Small Molecules with Multicolor Photoluminescence via a Host-Guest and Dual-Emission Strategy

Dengfeng Li,# Feifei Lu,# Jie Wang, Wende Hu, Xiao-Ming Cao, Xiang Ma* and He Tian

Key Laboratory for Advanced Materials and Institute of Fine Chemicals, Center for Computational Chemistry and Research Institute of Industrial Catalysis, School of Chemistry and Molecular Engineering, East China University of Science and Technology, Shanghai 200237, P. R. China

ABSTRACT: Metal-free room-temperature phosphorescence (RTP) materials offer unprecedented potentials for photoelectric and biochemical materials due to their unique advantages of long lifetime and low-toxicity. However, the achievements of phosphorescence at ambient condition so far have been mainly focused on ordered crystal lattice or on embedding into rigid matrices, where the preparation process might bring out poor repeatability and limited application. In this research, a series of amorphous organic small molecular compounds were developed with efficient room-temperature phosphorescence (RTP) emission through conveniently modifying phosphor moieties to β-cyclodextrin (β-CD). The hydrogen bonding between the cyclodextrin derivatives immobilizes the phosphors to suppress the non-radiative relaxation and shields phosphors from quenchers, which enables such molecules to emit efficient RTP emission with decent quantum yields. Furthermore, one of such cyclodextrin derivatives was utilized to construct a host-guest system incorporating a fluorescent guest molecule, exhibiting excellent RTP-fluorescence dual-emission properties and multicolor emission with a wide range from yellow to purple including the white-light emission. This innovative and universal strategy opens up new research paths to construct amorphous metal-free small molecular RTP materials and to design organic white-light emitting materials using a single supramolecular platform.

INTRODUCTION

Room-temperature phosphorescence (RTP) materials have attracted significant research interest due to their distinctive properties such as long decay lifetimes and the involvement of triplet states,[1] which have been applied widely in organic light-emitting diodes (OLED),[2-4] chemical sensors,[5-6] bio-imaging,[7-8] and molecular switches.[9-10] Generally, most RTP materials are inorganic or organometallic complexes containing noble metals. Considering their expenses and toxicity, it is indispensable to develop metal-free RTP materials with low cost, versatile molecular design and good processability. However, it is diffcult for these materials to emit efficient RTP signals, since the energy of the excited triplet states of organic molecules could be easily lost through thermally vibrational and collisional process or the exposure to the quenchers such as oxygen. Therefore, the promotion of intersystem crossing (ISC) efficiency and the suppression of the non-radiative relaxation process predominate in the construction of pure organic RTP materials.[11] Based on the aforementioned principles, several methods have already been developed including the embedding of organic phosphors into solid substrate,[12] silica glass,[13] polymer matrix,[14-16] and the cavity of macrocycle hosts.[17-20] RTP emission could also be enhanced by embedding the phosphor into poly (vinyl alcohol) (PVA)[21] or poly (methyl methacrylate) (PMMA)[22] to suppress the vibrational dissipation. Amorphous rigid steroidal compounds have also been applied to minimize the quenching of long-lived triplet excited states and to achieve efficient phosphorescence in pure organic amorphous guest materials in air.[23-25] Recently, a unique pure organic amorphous RTP system was developed by a simple radical polymerization of acrylamide and organic phosphors without extra processing, which could generate efficient RTP emission.[26] Until now, the research of pure organic compounds emitting RTP have focused mainly on crystallization-induced phosphorescence due to the rigid framework for phosphor to retard its molecular motion.[27-31] However, the demanding growth condition along with the uncontrollable growth process has greatly limited the development and application of the metal-free RTP materials constructed from crystallization. This indicates the centrality in designing and developing a convenient and applicable strategy to obtain amorphous organic small molecular compounds with efficient RTP emission.

Herein, we described a general design approach to develop amorphous metal-free organic single compounds with efficient RTP emission by modifying different phosphors onto β-CD, which could effectively suppress the non-radiative relaxation process and enhance the quantum yield. Strong intermolecular hydrogen bonding between cyclodextrins (CDs) restricts the vibration of phosphors and shields phosphorescent moieties from quenchers. Till now, such non-crystalline metal-free small compounds with efficient RTP emission have not been reported. Additionally, the cavity of β-CD was utilized to incorporate small fluorescent molecules to construct supramolecular system to engender multicolor emission including white-light one which was realized through a fluoroscence-phosphorescence dual-emission strategy.

RESULT AND DISCUSSION

To confirm the applicability of this approach, four different CD derivatives were prepared which were modified respectively by 6-bromo-2-naphthol (6-BrNp), 4-bromo-4'-hydroxybiphenyl (4-BrHB), 4-(4-bromophenyl)-pyridine (4-BrBp) and 4-bromo-1,8-napththalic anhydride (4-BrNpA) (Figure S1, Supporting Information). The structures of these four compounds were shown in Figure 1.

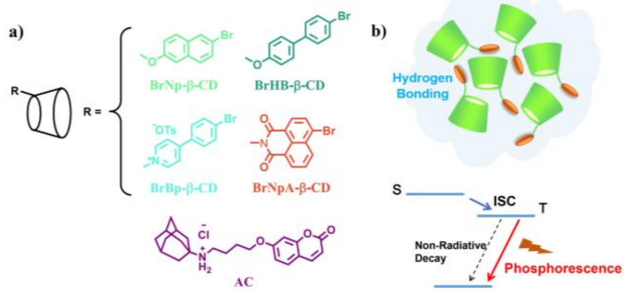

Figure 1. a) Molecular structures of RTP emissive cyclodextrin derivatives (**BrNp-β-CD**, **BrHB-β-CD**, **BrBp-β-CD** and **BrNpA-β-CD**) and fluorescent guest molecule **AC**; b) schematic illustration of the phosphorescence emission.

Synthesis. Mono[6-O-(4-methyl-phenylsulfonyl)]-β-cyclodextrin (6-OTs-β-CD) or 6-amino-β-cyclodextrin (6-NH_2-β-CD) was reacted with the organic phosphorescent functional groups to yield RTP-emissive cyclodextrin derivatives. The guest molecule AC was obtained through alkylation coupling between coumarin and amantadine and subsequent protonation by hydrochloric acid.

Photophysical properties of CD derivatives. As anticipated, a strong RTP emission was observed from the four CD derivatives in the amorphous solid state. Their fluorescence emissions were weak because of the heavy-atom effect from the Br substitutes. As shown in Figure 2, the BrNp-β-CD powder emitted visible yellow-green light under 254 nm UV light with decent phosphorescent quantum yields (5.9%). The RTP emission spectrum revealed that BrNp-β-CD was excited to generate a strong emission peak at about 512 nm and 537 nm (Figure 2). The lifetime of the emission peak at 512 nm reached 1.85 ms, which further verified the RTP emission (Figure S3). The other three compounds showed similar properties with BrNp-β-CD and their photophysical data were collected in Table 1. Comparing the phosphorescence excitation spectra (Figure S4), we found that the Stokes shifts of RTP emission reached over 230 nm for BrNp-β-CD, 220 nm for BrNpA-β-CD, 200 nm for both BrHB-β-CD and BrBp-β-CD, respectively, which manifested their RTP emission characteristics. Moreover, the X-ray powder diffraction (XRD) was used to explore the microstructure of these compounds. The results showed there was no significant crystal characteristics, verifying their amorphous states (Figure 3). It could be safely estimated that these pure organic compounds are RTP emissive in the amorphous solid state rather than in the solution or crystalline state, which makes them convenient for both preparation and practical application.

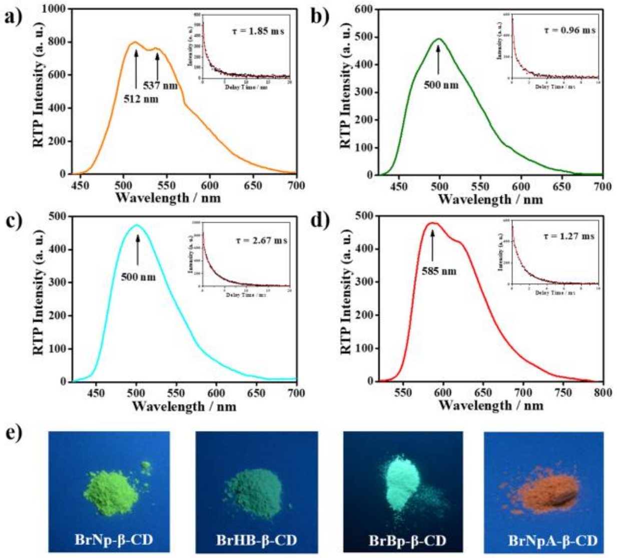

Figure 2. RTP emission spectra of a) **BrNp-β-CD**, b) **BrHB-β-CD**, c) **BrBp-β-CD** and d) **BrNpA-β-CD** (phosphorescence mode; excitation slim =10 nm; emission slim =10 nm; excitation wavelength of a) 285 nm, b) 300 nm), c) 350 nm, d) 365 nm) in solid state. Inset: luminescent delay lifetimes of a) **BrNp-β-CD** at 512 nm, b) **BrHB-β-CD** at 500 nm, c) **BrBp-β-CD** at 500 nm and d) **BrNpA-CD** at 585 nm. Photographs of the solid powder of e) **BrNp-β-CD**, **BrHB-β-CD, BrBp-β-CD** under 254 nm UV light and **BrNpA-β-CD** under 365 nm UV light.

Mechanism analysis for the enhancement of RTP emission. The previous reports revealed that the orientation of phosphorescent emission at room temperature could be attributed to both the internal factors such as the molecular structure design for efficient

Table 1. Photophysical data of **BrNp-β-CD**, **BrHB-β-CD**, **BrBp-β-CD** and **BrNpA-β-CD**.

Compound	λ_{ex} [nm]	λ_{em} [nm]	τ_p [ms]	Φ_p [%]
BrNp-β-CD	285, 327	512, 537	1.85	5.9
BrHB-β-CD	300	500	0.96	2.8
BrBp-β-CD	340	500	2.67	16.9
BrNpA-β-CD	365	585	1.27	1.0

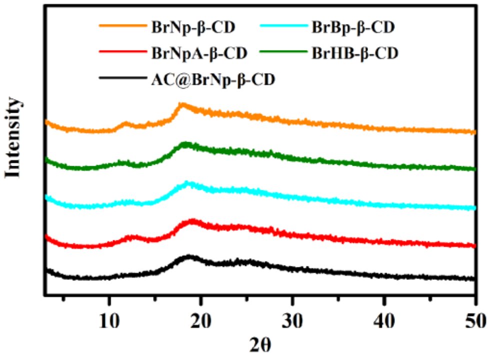

Figure 3. X-ray powder diffraction (XRD) patterns of **BrNp-β-CD**, **BrHB-β-CD**, **BrBp-β-CD** and **AC@BrNp-β-CD** powder (molar ratio **AC**: **BrNp-β-CD** = 1:1).

spin-orbital coupling[32] and the external factors such as the environmental matrix for the suppression of non-radiative decay.[15] Furthermore, it could be inferred that cyclodextrin was least likely to promote the ISC process, since, without its unsaturated group, it could hardly participate in the electron transition process. To confirm the influence of cyclodextrin unit on the enhanced RTP emission in this system, (TD)-B3LYP/6-311+G* calculations were implemented to study the phosphors and four CD derivatives in the amorphous state. Figure 4 and Figure S5 showed that the frontier molecular orbits of CD derivatives and their corresponding phosphors mainly concentrated on the phosphor moieties, indicating that CD was not involved in the efficient spin-orbital coupling. More was found through comparing the energy levels of the singlet and triplet excited states of the phosphors and the coupled CD derivatives that the energy gap (ΔE_{ST}) between S_1 and T_1 was nearly unchanged with a moderate value, which was favorable for the ISC process.[33] This highlighted the critical role of the matrix roles in the process of RTP emission. The potential hydrogen bonding environment was also studied to develop insights into the matrix part and the hydroxy group around the CD molecules. The hydrogen bonding between the adjacent CDs might immobilize the phosphorescent moieties to suppress the vibrational dissipation and provide a secluded environment away from oxygen to a certain degree. Since the hydrogen bond could be broken during dissolution in the relatively polar solvent, an N, N-dimethylformamide/ethyl acetate (DMF/EA) mixed soluble/insoluble solvent system was applied to study the effect. Specific concentration of BrNp-β-CD suspension (0.3 mg/mL) was prepared with different ratios of the mixed solvents ranging from 0 to 0.3 (volume ratio). As shown in Figure 5, the RTP emission decreased remarkably with the increase of the DMF content when it was irradiated with 254 nm light. Similar characters applied to BrHB-β-CD, BrBp-β-CD and BrNpA-β-CD, which demonstrated the conclusion above. Besides, 6-BrNp was mixed with its equivalent of β-CD and methyl-β-cyclodextrin (Me-β-CD) in DMF respectively before their powder was collected in vacuum. 6-BrNp embedded with β-CD still exhibited obvious phosphorescent emission due to the existence of hydrogen bond between cyclodextrins. However, the RTP emission of 6-BrNp became weak when embedded with

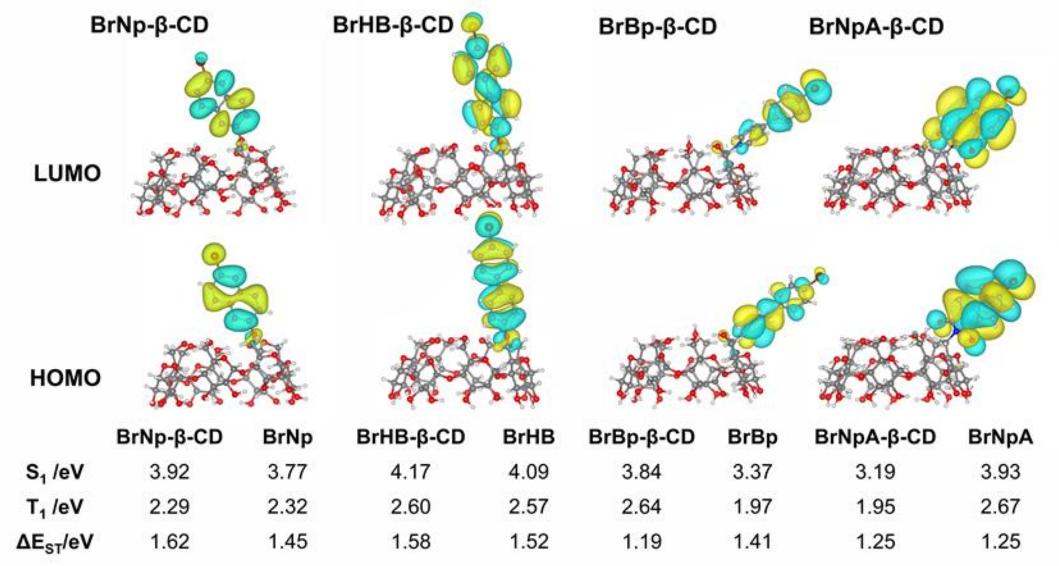

	BrNp-β-CD	BrNp	BrHB-β-CD	BrHB	BrBp-β-CD	BrBp	BrNpA-β-CD	BrNpA
S_1 /eV	3.92	3.77	4.17	4.09	3.84	3.37	3.19	3.93
T_1 /eV	2.29	2.32	2.60	2.57	2.64	1.97	1.95	2.67
ΔE_{ST}/eV	1.62	1.45	1.58	1.52	1.19	1.41	1.25	1.25

Figure 4 Calculated HOMO and LUMO for the ground states and calculated energies for excited singlet state (S_1), excited triplet state (T_1) and ΔE_{ST} for CD derivatives **BrNp-β-CD, BrHB-β-CD, BrBp-β-CD** and **BrNpA-β-CD**.

Me-β-CD (Figure 6a). By analyzing the phosphorescence properties listed in Figure 6c, it could be deduced that the hydrogen bonding atmosphere might benefit the enhancement of the RTP emission by restricting the vibration of phosphors to suppress the non-radiative decay.

6-BrNp and β-CD in the aqueous solution could form a 1:1 inclusion complex 6-BrNp@β-CD with a relatively low constant of K_a = 840 M^{-1}, which would emit weak RTP signals.[34] Nevertheless, the pre-assembly of 6-BrNp with β-CD (6-BrNp@β-CD) in the aqueous solution would promote the densification of hydrogen bonding surrounding for phosphors in the solid state. Figure 6 showed that the solid inclusion complex emitted stronger RTP signals than in the random mixture. The 2D ROESY NMR spectrum of BrNp-β-CD (Figure S7) showed weak signals between the protons of 6-BrNp group and CD, which implied that 6-BrNp might enter into the cavity of CD. Therefore, it was also necessary to evaluate the influence of the host-guest interaction in this solid system. It is well known that the inclusion complexes formed by β-CD and guests are influenced by the solvent effect because of the hydrophobic property of the β-CD cavity[35-36] and normally instable in non-aqueous solution.[37] BrNp-β-CD was dissolved in dry DMF or H_2O, respectively, and then evaporated the solvents to get the samples in vacuum. Figure S7 depicted the RTP spectra of BrNp-β-CD powder obtained from the aqueous or non-aqueous solution under the same test conditions, which showed no obvious difference in their emission intensities. Therefore, the hydrogen bonding interaction dominates the enhancement of RTP intensity in our designed molecules in this research, ascribed to the steric hindrance obstructing the host-guest inclusion. With the aim of demonstrating the role of modification in the efficient RTP emission, the control experiments between BrNp-β-CD and the complex 6-BrNp@β-CD were implemented. In comparison with the emission intensity and the quantum yield, BrNp-β-CD manifested better RTP-emissive property superior to the complex (Figure 6b and 6c), which indicated that the covalent bonding from modification could preferably restrict the activity of phosphors to a great extent.

Application in multicolor materials including white-light emitting ones. The cavity of CD derivatives endows them with the ability to accommodate diverse guest molecules. Adamantane (AD) derivatives can form stable inclusion complexes with β-CD.[38-39] Based on the properties above, a simple host-guest system was hence developed, which consisted of BrNp-β-CD host and a linear fluorescent guest molecule AC containing an AD moiety and a coumarin unit at each end linked by a $(CH_2)_4$ alkyl chain. By mixing these two components in the aqueous solution, a host-guest complex AC@BrNp-β-CD was obtained because of the firm inclusion of AC in the cyclodextrin cavity of BrNp-β-CD. A job's plot by UV-Vis absorption spectroscopy was conducted, confirming that BrNp-β-CD and AC interacted in a 1:1 binding stoichiometry (Figure S8). ^{1}H NMR experiments were conducted to validate the inclusion behavior. As presented in Figure S9, there were three sets of protons in the AD moiety marked as H_a, H_b and H_c. With the addition of BrNp-β-CD, the ^{1}H NMR signals corresponding to these protons broadened. H_a proton shifted upfield ($\Delta\delta H_a$ = - 0.06 ppm) whilst H_b, H_c protons downfield ($\Delta\delta H_b$ = + 0.02 ppm, $\Delta\delta H_c$ = + 0.04 ppm). This indicated that H_a proton has been deeply included in the cavity while H_b, H_c protons remained at the periphery of the wider rim of BrNp-β-CD. This was consistent with the previously reported literature.[40] Furthermore, 2D ROESY NMR spectrum of the complex AC@BrNp-β-CD in D2O showed strong ROE signals between protons $H_{a\text{-}c}$ and BrNp-β-CD (Figure S10). Few other correlation signals were observed between the protons of other aromatic rings and BrNp-β-CD. It was definitely deduced that the cavity of BrNp-β-CD was only occupied by the AD moiety. Another evidence to confirm

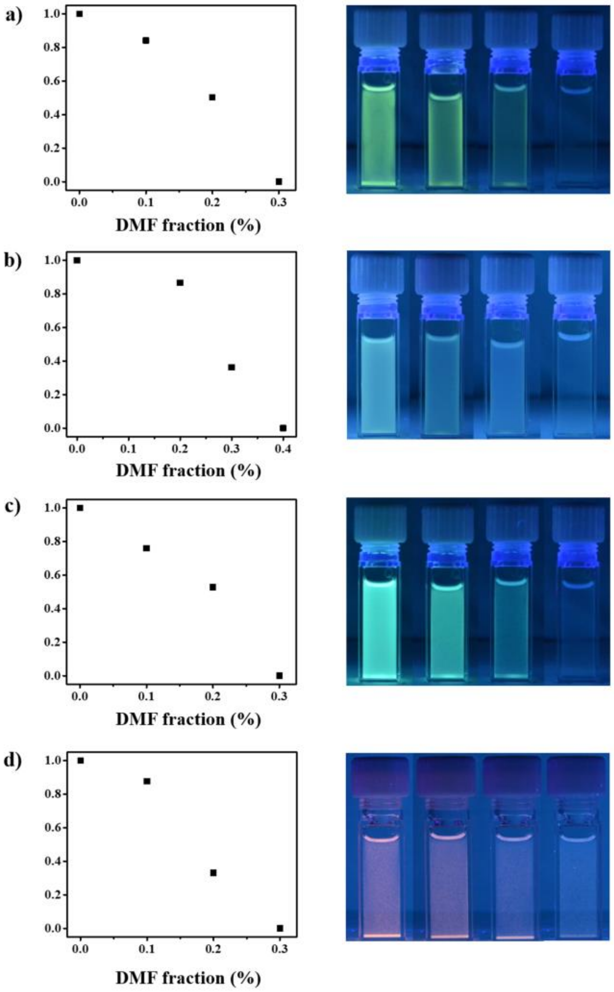

Figure 5. Normalized RTP intensities of a) **BrNp-β-CD** at 512 nm, b) **BrHB-β-CD** at 500 nm, c) **BrBp-β-CD** at 500 nm and d) **BrNpA-β-CD** at 585 nm at different volume mixing ratios of DMF/EA. The corresponding photographs of a) **BrNp-β-CD**, b) **BrHB-β-CD**, c) **BrBp-β-CD** under 254 nm irradiation and d) **BrNpA-β-CD** under 365 nm irradiation.

the formation of the 1:1 host-guest complex was supported by Matrix-Assisted Laser Desorption/Ionization Time of Flight Mass Spectrometry (MALDI-TOF-MS). A strong peak at 1708.5961 corresponding to [AC + BrNp-β-CD − Cl]$^+$ was observed, showing an ideal match between the calculated and measured mass peaks for the 1:1 host-guest complex (Figure S11).

As the demonstration of the actual formation of the inclusion complex in solution cannot persuasively guarantee its existence in the solid state, extra analytical techniques are necessary for the characterization of AC@BrNp-β-CD solid system, including FT-IR, TGA and SEM.[41-45] The FT-IR spectra of AC, BrNp-β-CD, the physical mixture PM (AC and BrNp-β-CD with molar ratio 1:1) and solid inclusion complex AC@BrNp-β-CD are shown in Figure S12. For AC, the stretching frequencies of N-H and C-H belonging to AD were observed in 3436.11 cm^{-1} and 2919.84 cm^{-1}, respectively. However, most of them diminished in intensity or even disappeared in AC@BrNp-β-CD, suggesting that AC was involved into the inclusion process. In contrast, the subtle characteristic peaks of AC and BrNp-β-CD were shown on the FT-IR spectrum of PM, which could be regarded as a simple superimposition of the host and guest molecule. TGA curves in Figure S13 showed mass losses indicating the following orders of the thermal stability of the samples: BrNp-β-CD > AC@BrNp-β-CD > PM > AC. Compared with AC (ca. 226 °C), the fact that a higher decomposition temperature (ca. 256 °C) needed for AC@BrNp-β-CD suggests the formation of the inclusion complex. SEM helps to evidence the morphological changes related to the interactions between the components in the solid inclusion complexes. As shown in Figure S14, the SEM images of BrNp-β-CD, AC, PM and AC@BrNp-β-CD revealed a completely different shape and size between AC@BrNp-β-CD and PM, which reflected the formation of solid inclusion complex.

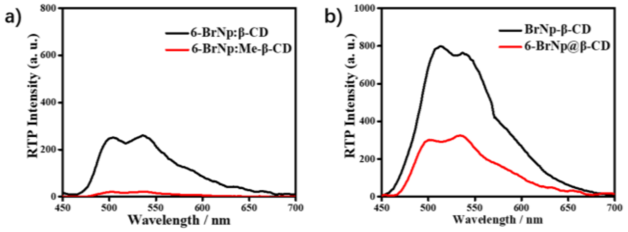

c)

	BrNp-β-CD	6-BrNp@β-CD	6-BrNp:β-CD	6-BrNp:Me-β-CD
τ_p(ms)	1.85	1.69	1.65	1.54
Φ_p(%)	5.9	2.9	1.0	<0.1

Figure 6. RTP emission spectra of a) mixtures 6-BrNp: β-CD and 6-BrNp:Me-β-CD (molar ratio 1:1) powder prepared from DMF solution and b) BrNp-β-CD and the complex 6-BrNp@β-CD (1:1) powder obtained from mixed solution (ethanol (v): H$_2$O (v) = 1:9). c) RTP lifetime (τ_p) and quantum yield (Φ_p) of solid samples mentioned above. Excitation voltage for a) 600 V, b) 500 V; excitation slim = 10 nm; emission slim = 10 nm; excited at 285 nm.

To investigate the optical properties of this complex, the absorption spectra were measured in an aqueous solution. Figure S15 depicted the absorption spectra of BrNp-β-CD, AC and AC@BrNp-β-CD as well as the reference compound 6-BrNp. The spectrum of AC@BrNp-β-CD showed the three sets of characteristic absorption peaks at around 235 nm, 275 nm and 325 nm, which belonged to the chromophore pieces contained in AC@BrNp-β-CD compared with the reference compound 6-BrNp and AC. A more careful comparison revealed that the intensity of the absorption peaks assigned to 6-BrNp moiety increases due to the competitive inclusion of AC. PL spectroscopy studies of AC@BrNp-β-CD assembled in different ratio of two components in the solid state were carried out. The PL spectra of the solid inclusion complex

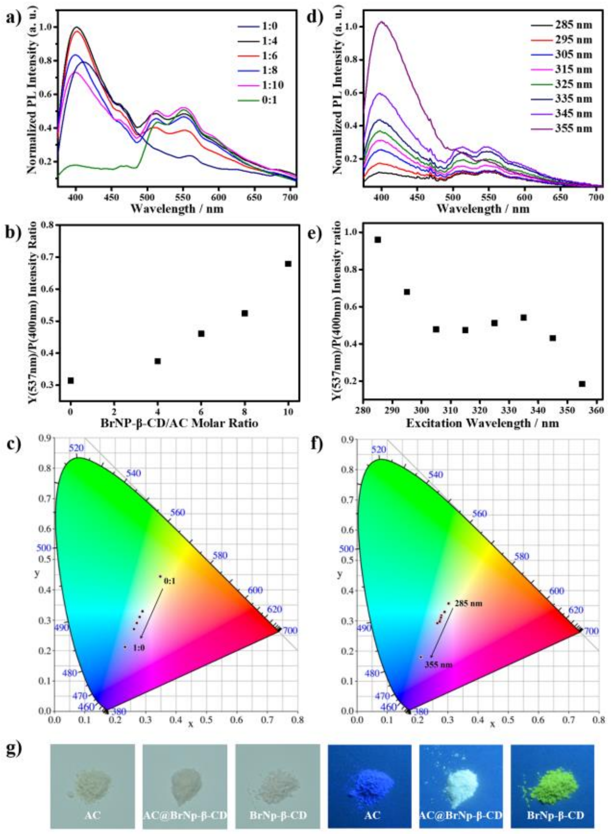

Figure 7. a) PL emission spectra of **AC@BrNp-β-CD** (different molar ratio **BrNp-β-CD**:**AC**); b) the yellow/purple (Y/P) emission intensity ratio and c) calculated PL emission color coordinates of **AC@BrNp-β-CD** in the CIE 1931 chromaticity diagram as a function of **BrNp-β-CD**:**AC** (molar ratio 0:1, 4:1, 6:1, 8:1 and 10:1, respectively). d) PL emission spectra of **AC@BrNp-β-CD** (molar ratio **BrNp-β-CD**:**AC** =10:1, using different excitation wavelength), e) the yellow/purple (Y/P) emission intensity ratio and f) calculated PL emission color coordinates in the CIE 1931 chromaticity diagram as a function of excitation wavelength (285, 295, 305, 315, 325, 335, 345 and 355 nm); g) photographs of **AC**, **AC@BrNp-β-CD** and **BrNp-β-CD** under daylight and UV irradiation, respectively. All the measurements were carried out in the solid state.

AC@BrNp-β-CD were found to show noticeable broad dual emission peaks, recognized as the emission of coumarin group at 400 nm (blue-purple band) and the BrNp group emission at 512 nm and 537 nm (yellow-green band) (Figure 7). As showed in Figure S16, the blue-purple emission is excited at 330 nm, whereas the excitation for the yellow-green emission was at 285 nm and 327 nm. Furthermore, the PL emission of the solid powder of AC was found to emit at 400 nm when excited at 360 nm. On the basis of the PL spectra above, it could be legitimately inferred that the dual emissions of AC@BrNp-β-CD originate from AC and BrNp-β-CD.

Additionally, how to modulate the PL emission was also investigated by tuning the molar ratio of the two components AC and BrNp-β-CD or by turning the excitation wavelength. The pre-organization of BrNp-β-CD:AC with different molar ratios generated a series of powder with muticolor emission (including white-light one) under the UV irradiation. The emission spectroscopy studies revealed that the intensity of the yellow-green band increased gradually at the expense of the intensity of the blue-purple band as a function of BrNp-β-CD:AC (Figure 7). The variation of excitation wavelength led to different emissions of the host-guest complex. When BrNp-β-CD was excited using the light above 350 nm, its RTP emission became negligible. Similar results could be observed in the complex consisting of BrNp-β-CD and AC, which primarily emitted the blue-purple light emission upon light irradiation at 365 nm. When excited at diverse excitation wavelengths, the PL emission of the complex with different ratios corresponding to a CIE coordinate and the values were collected in Table S1. Interestingly, almost pure white-light emission with the CIE coordinates calculated as (0.29, 0.33) was realized when BrNp-β-CD incorporated with 0.1 equivalent of AC under the excitation at 295 nm (Figure 7). Ascribed to the modest water solubility, BrNp-β-CD was sensitive to ambient humidity and hence emitted intensity-variable RTP when dispersed into the different ratios of DMF/H_2O solution (Figure S17). AC@BrNp-β-CD retained the properties of AC and also showed responsiveness to the moisture, which was promising for humidity detection.

Conclusion

An innovative strategy was presented in this research to construct amorphous metal-free RTP small molecular compounds by modifying phosphors to β-CD. These amorphous β-CD derivatives emitted strong RTP luminescence with decent quantum yields. This approach possessed the strengths of convenient preparation, feasibility and universality, low-nontoxicity, phosphorescence emission without the rigorous requirements for de-oxygenization and low temperature. Moreover, BrNp-β-CD was utilized to construct a host-guest system with another water-soluble coumarin derivative. Compared with the previously reported white-light emitting materials,[46-48] this type of complexes combined RTP-emissive macrocycle molecules with fluorescent guest ones to successfully generate white-light emission by using the host-guest interaction. Additionally, this system exhibits unique dual emission bands in the solid state. It can be modulated in a dual model by altering the proportion of BrNp-β-CD and AC and the excitation wavelength, which may contribute to the prospect of the multicolor emitting materials.

ASSOCIATED CONTENTS

Supporting Information. The detailed experiments, computational simulation and additional spectroscopic data. This material is available at http://pubs.acs.org.

AUTHOR INFORMATION

Corresponding Author

* maxiang@ecust.edu.cn

Author Contributions

[#] These two authors (D. Li and F. Lu) contributed equally to this work.

ACKNOWLEDGMENT

We gratefully acknowledge the financial support from NSFC/China (21788102, 21722603, 214210004, 21476075 and 21790361), Programme of Introducing the Talents of Discipline to Universities (B16017), Innovation Program of Shanghai Municipal Education Commission and the Fundamental Research Funds for the Central Universities (WJ1514309 and 222201717003). The authors also thank Miss J. Wu for helping draw figures, Dr. Q. Zhang and Dr. H. Chen for helpful discussions, and Dr. X. Rao for refining the manuscript.

REFERENCES

(1) (a) Baldo, M. A.; O'Brien, D. F.; You, Y.; Shoustikov, A.; Sibley, S.; Thompson, M. E.; Forrest, S. R. *Nature* **1998**, 395, 151-154. (b) Baldo, M. A.; Thompson, M. E.; Forrest, S. R. *Nature* **2000**, 403, 750-753. (c) Wei, Y.; Shuang, S.; Dong, C.; Jin, W.; Gao, C.; Wei, Y.; Liu, C. *Trends. Appl. Spectrosc.* **2004,** *5*, 195-224.

(2) Tao, Y.; Wang, Q.; Yang, C.; Wang, Q.; Zhang, Z.; Zou, T.; Qin, J.; Ma, D. *Angew. Chem. Int. Ed.* **2008,** *47*, 8104-8107.

(3) Chang, C.-F.; Cheng, Y.-M.; Chi, Y.; Chiu, Y.-C.; Lin, C.-C.; Lee, G.-H.; Chou, P.-T.; Chen, C.-C.; Chang, C.-H.; Wu, C.-C. *Angew. Chem. Int. Ed.* **2008,** *47*, 4542-4545.

(4) Xiao, L.; Su, S.-J.; Agata, Y.; Lan, H.; Kido, J. *Adv. Mater.* **2009,** *21*, 1271-1274.

(5) Melaimi, M.; Gabbaie, F. P. *J. Am. Chem. Soc.* **2005,** *127*, 9680-9681.

(6) Ipe, B. I.; Yoosaf, K.; Thomas, K. G. *J. Am. Chem. Soc.* **2006,** *128*, 1907-1913.

(7) Zhao, Q.; Huang, C.; Li, F. *Chem. Soc. Rev.* **2011,** *40*, 2508-2524.

(8) Shiu, H.-Y.; Chong, H.-C.; Leung, Y.-C.; Zou, T.; Che, C.-M. *Chem. Commun.* **2014,** *50*, 4375-4378.

(9) Monaco, S.; Semeraro, M.; Tan, W.; Tian, H.; Ceroni, P.; Credi, A. *Chem. Commun.* **2012,** *48*, 8652-8654.

(10) Ma, X.; Zhang, J.; Cao, J.; Yao, X.; Cao, T.; Gong, Y.; Zhao, C.; Tian, H. *Chem. Sci.* **2016,** *7*, 4582-4588.

(11) (a) Baryshnikov, G.; Minaev, B.; Ågren, H. *Chem. Rev.* **2017**, 117, 6500-6537. (b) Liu, Y.; Zhan, G.; Liu, Z.-W.; Bian, Z.-Q.; Huang, C.-H. *Chin. Chem. Lett.* **2016,** *27*, 1231-1240.

(12) Asafu-Adjaye, E. B.; Su, S. Y. *Anal. Chem.* **1986,** *58*, 539-543.

(13) Kaufman, V. R.; Levy, D.; Avnir, D. *J. Non-Cryst. Solids* **1986,** *82*, 103-109.

(14) Pang, Z.; Gu, X.; Yekta, A.; Masoumi, Z.; Coll, J. B.; Winnik, M. A.; Manners, I. *Adv. Mater.* **1996,** *8*, 768-771.

(15) Kwon, M. S.; Yu, Y.; Coburn, C.; Phillips, A. W.; Chung, K.; Shanker, A.; Jung, J.; Kim, G.; Pipe, K.; Forrest, S. R.; Youk, J. H.; Gierschner, J.; Kim, J. *Nat. Commun.* **2015,** *6*, 8947.

(16) Baroncini, M.; Bergamini, G.; Ceroni, P. *Chem. Commun.* **2017,** *53*, 2081-2093.

(17) Chen, H.; Ma, X.; Wu, S.; Tian, H. *Angew. Chem. Int. Ed.,* **2014**, 53, 14149-14152.

(18) Cao, J.; Ma, X.; Min, M.; Cao, T.; Wu, S.; Tian, H. *Chem. Commun.* **2014,** 50, 3224-3226.

(19) Gong, Y.; Chen, H.; Ma, X.; Tian, H. *ChemPhysChem.* **2016,** *17*, 1934-1938.

(20) Chen, H.; Xu, L.; Ma, X.; Tian, H. *Polym. Chem.* **2016**, 7, 3989-3992.

(21) Kwon, M. S.; Lee, D.; Seo, S.; Jung, J.; Kim, J. *Angew. Chem. Int. Ed.* **2014,** *53*, 11177-11181.

(22) Lee, D.; Bolton, O.; Kim, B. C.; Youk, J. H.; Takayama, S.; Kim, J. *J. Am. Chem. Soc.* **2013,** *135*, 6325-6329.

(23) Hirata, S.; Totani, K.; Zhang, J.; Yamashita, T.; Kaji, H.; Marder, S. R.; Watanabe, T.; Adachi, C. *Adv. Funct. Mater.* **2013,** *23*, 3386-3397.

(24) Katsurada, Y.; Hirata, S.; Totani, K.; Watanabe, T.; Vacha, M. *Adv. Opt. Mater.* **2015,** *3*, 1726-1737.

(25) Hirata, S.; Vacha, M. *J. Phys. Chem. Lett.* **2016,** *7*, 1539-1545.

(26) Chen, H.; Yao, X.; Ma, X.; Tian, H. *Adv. Opt. Mater.* **2016,** *4*, 1397-1401.

(27) Yuan, W. Z.; Shen, X. Y.; Zhao, H.; Lam, J. W. Y.; Tang, L.; Lu, P.; Wang, C.; Liu, Y.; Wang, Z.; Zheng, Q.; Sun, J. Z.; Ma, Y.; Tang, B. Z. *J. Phys. Chem. C.* **2010,** *114*, 6090-6099.

(28) Bolton, O.; Lee, K.; Kim, H.-J.; Lin, K. Y.; Kim, J. *Nat. Chem.* **2011,** *3*, 205-210.

(29) Gong, Y.; Chen, G.; Peng, Q.; Yuan, W. Z.; Xie, Y.; Li, S.; Zhang, Y.; Tang, B. Z. *Adv. Mater.* **2015,** *27*, 6195-6201.

(30) Yang, Z.; Mao, Z.; Zhang, X.; Ou, D.; Mu, Y.; Zhang, Y.; Zhao, C.; Liu, S.; Chi, Z.; Xu, J.; Wu, Y. C.; Lu, P. Y.; Lien, A.; Bryce, M. R. *Angew. Chem. Int. Ed.* **2016,** *55*, 2181-2185.

(31) Yang, J.; Ren, Z.; Xie, Z.; Liu, Y.; Wang, C.; Xie, Y.; Peng, Q.; Xu, B.; Tian, W.; Zhang, F.; Chi, Z.; Li, Q.; Li, Z. *Angew. Chem. Int. Ed.* **2017,** *129*, 898-902.

(32) Zhao, W.; He, Z.; Lam, Jacky W. Y.; Peng, Q.; Ma, H.; Shuai, Z.; Bai, G.; Hao, J.; Tang, B. Z. *Chem.* **2016,** *1*, 592-602.

(33) Ma, H.; Shi, W.; Ren, J.; Li, W.; Peng, Q.; Shuai, Z. *J. Phys. Chem. Lett.* **2016,** *7*, 2893-2898.

(34) Zhai, Y.-Q.; Zhang, S.-Z.; Xie, J.-W.; Liu, C.-S. *Anal. Chim. Acta.* **2003,** *494*, 71-80.

(35) Eftink, M. R.; Harrison, J. C. *Bioorg. Chem.* **1981,** *10*, 388-398.

(36) Bortolus, P.; Monti, S. *J. Phys. Chem.* **1987,** *91*, 5046-5050.

(37) Liu, Y.; Zhao, Y.-L.; Zhang, H.-Y.; Fan, Z.; Wen, G.-D.; Ding, F. *J. Phys. Chem. B.* **2004,** *108*, 8836-8843.

(38) Rekharsky, M. V.; Inoue, Y. *Chem. Rev.* **1998,** *98*, 1875-1918.

(39) Liu, Y.; Yu, Z.-L.; Zhang, Y.-M.; Guo, D.-S.; Liu, Y.-P. *J. Am. Chem. Soc.* **2008,** *130*, 10431-10439.

(40) (a) Miyauchi, M.; Harada, A. *J. Am. Chem. Soc.* **2004**, 126, 11418-11419. (b) Tao, W.; Liu, Y.; Jiang, B.; Yu, S.; Huang, W.; Zhou, Y.; Yan, D. *J. Am. Chem. Soc.* **2012**, 134, 762-764. (c) Krishnan, R.; Rakhi, A. M.; Gopidas, K. R. *J. Phys. Chem. C* **2012,** *116*, 25004-25014.

(41) Yang, L.-J.; Chen, W.; Ma, S.-X.; Gao, Y.-T.; Huang, R.; Yan, S.-J.; Lin, J. *Carbohydr. Polym.* **2011,** *85*, 629-637.

(42) Garnero, C.; Aiassa, V.; Longhi, M. *J. Pharm. Biomed. Anal.* **2012,** *63*, 74-79.

(43) Mora, M. J.; Tártara, L. I.; Onnainty, R.; Palma, S. D.; Longhi, M. R.; Granero, G. E. *Carbohydr. Polym.* **2013,** *98*, 380-390.

(44) Mura, P. *J. Pharm. Biomed. Anal.* **2015,** *113*, 226-238.

(45) Rajamohan, R.; Nayaki, S. K.; Swaminathan, M. *J. Mol. Liq.* **2016,** *220*, 918-925.

(46) Zhang, Z.; Wu, Y. S.; Tang, K. C.; Chen, C. L.; Ho, J. W.; Su, J.; Tian, H.; Chou, P. T. *J. Am. Chem. Soc.* **2015,** *137*, 8509-8520.

(47) Zhang, Q. W.; Li, D.; Li, X.; White, P. B.; Mecinović, J.; Ma, X.; Ågren, H.; Nolte, R. J. M.; Tian, H. *J. Am. Chem. Soc.* **2016,** *138*, 13541-13550.

(48) Ni, X.-L.; Chen, S.; Yang, Y.; Tao, Z. *J. Am. Chem. Soc.* **2016,** *138*, 6177-6183.

Table of Contents artwork